UDK 528.481:624.131.535:691.22(513)
Original scientific article/Izvirni znanstveni članek

ISSN 1580-2949
MTAEC9, 55(5)741(2021)

EXPERIMENTAL STUDY ON THE DYNAMIC SHEAR MODULUS AND DAMPING RATIO OF SATURATED SAND UNDER CYCLIC LOADING

EKSPERIMENTALNA ŠTUDIJA DINAMIČNEGA STRIŽNEGA MODULA IN DUŠILNEGA RAZMERJA Z VLAGO NASIČENEGA PESKA V POGOJIH DINAMIČNEGA OBREMENJEVANJA

Jian Zhang[1*], Jiuting Cao[2], Sijie Huang[3], Baocun Shi[4]

[1]Nanjing Vocational Institute of Transport Technology, Nanjing 211188, China
[2]Jiangsu Zhongshe Group Co., Ltd., Wuxi 214072, China
[3]Tianjin Research Institute for Water Transport Engineering, Tianjin 300456, China
[4]Hohai University, Nanjing 210098, China

Prejem rokopisa – received: 2021-07-27; sprejem za objavo – accepted for publication: 2021-08-19

doi:10.17222/mit.2021.230

Initial shear stress is inevitable in actual engineering slopes, subgrades and foundations, and soils exhibit different dynamic characteristics under the influence of initial shear stress. Using a dynamic triaxial test system, this study explores the dynamic shear modulus and damping ratio of saturated sand from Wenchuan, investigates the effects of the initial shear stress and vibration frequencies on the dynamic shear modulus and damping ratio of saturated sand and proposes a normalised dynamic shear modulus formula that considers the initial shear stress and vibration frequency. Results show a threshold dynamic shear strain of the saturated sand. When the dynamic shear strain is below this threshold, the dynamic shear modulus significantly increases with the initial shear stress and vibration frequency. Otherwise, the influence of the initial shear stress and vibration frequency gradually decreases and eventually stabilises. The initial shear stress significantly affects the normalised dynamic shear modulus/strain curves where a larger initial shear stress corresponds to a higher curve. Meanwhile, the vibration frequency only exerts a slight influence. The curves under different frequencies are generally within the same band and fall near the Seed upper envelope. The initial shear stress also has a significant influence on the damping ratio where a larger initial shear stress corresponds to a smaller damping ratio. On the basis of the experimental results, a normalised dynamic shear modulus/shear strain formula that considers the influence of the initial shear stress and vibration frequency is established. Fitting results indicate that this formula shows good agreement with the test data.

Keywords: initial shear stress, saturated sand, dynamic shear modulus, damping ratio

Z začetno strižno napetostjo se neizogibno srečamo, ko obravnavamo probleme vezane na inženirske hribine, strmine, nagibe, podzemelja in temelje. Vsi ti objekti različno dinamično reagirajo pod vplivom začetne strižne napetosti. Avtorji tega članka so uporabili sistem za dinamično obremenilno triosno testiranje. V študiji so raziskovali dinamični strižni modul in dušilno razmerje z vlago nasičenega peska oz. zemljine iz Wenchuana, provinca Sichuan na Kitajskem (potres 2008). Raziskovali so vpliv učinka začetne strižne napetosti in vibracijskih frekvenc na dinamični strižni modul in dušilno razmerje z vlago nasičenega peska ter predlagali formulo za normalizirani dinamični strižni modul, ki upošteva začetno strižno napetost in vibracijsko frekvenco. Rezultati raziskave so dali mejno (maksimalno) dinamično strižno deformacijo v nasičenem pesku. Ko je dinamična strižna deformacija pod mejno vrednostjo, dinamični strižni modul močno narašča vzdolž začetne strižne napetosti in vibracijske frekvence. Sicer pa začetna strižna napetost in vibracijska frekvenca postopoma padata in se eventualno stabilizirata. Začetna strižna napetost pomembno vpliva na potek krivulj normaliziranega strižnega modula v odvisnosti od deformacije, pri tem pa večja začetna strižna napetost odgovarja višjim krivuljam, medtem ko vibracijska frekvenca kaže le rahel vpliv. Krivulje so za različne frekvence v splošnem znotraj istega pasu in padejo blizu Seedovega zgornjega ovoja. Začetna strižna napetost ima tudi pomemben vpliv na dušilno razmerje in večja kot je začetna strižna napetost, manjše je dušilno razmerje. Medtem ko ima vibracijska frekvenca nanj le manjši vpliv. Avtorji so, na osnovi eksperimentalnih rezultatov, podali formulo za odvisnost med normaliziranim strižnim modulom in strižno deformacijo, ki upošteva vpliv začetne strižne napetosti in vibracijske frekvence. Prilagajanje ("fitanje") podatkov kaže na to, da se izračuni s to formulo dobro ujemajo z eksperimentalnimi rezultati.

Ključne besede: začetna strižna napetost, z vlago nasičen pesek, dinamični strižni modul, dušilno razmerje

1 INTRODUCTION

As two important parameters that describe the dynamic properties of soil, the dynamic shear modulus and damping ratio serve as the basis for analysing the dynamic response of the soil-structure interaction under dynamic load and are the prerequisites considered for a dynamic analysis using numerical methods.[1–5] Many experimental investigations[6–8] of sand using cyclic triaxial tests reveal that a small strain shear modulus G_{max} is related to void ratio e and mean principal stress σ_m when the shear strain amplitude is $\gamma < 10^{-5}$. Hardin and Richart[9] computed such a modulus as

$$G_{max} = AF(e)(\sigma'_m)^n \quad (1)$$

where A and n refer to the soil fabric formed through various stress and strain histories, σ_m denotes the mean effective principle stress and $F(e)$ is the function of void ratio that is computed as

*Corresponding author's e-mail:
18626439990@163.com (Jian Zhang)

$$F(e) = \frac{(2.973 - e)^2}{(1 + e)} \quad (2)$$

Hardin and Richart computed the maximum dynamic shear modulus of round and angular grain sands when $\gamma < 10^{-4}$ as

$$G_{max} = 7000 \frac{(2.17 - e)^2}{(1 + e)} \sigma'^{0.5}_m \quad (3)$$

$$G_{max} = 3300 \frac{(2.97 - e)^2}{(1 + e)} \sigma'^{0.5}_m \quad (4)$$

Seed and Idriss[10] formulated the maximum dynamic shear modulus of sand as follows whilst considering the effects of the shear strain and mean effective principal stress:

$$G_{max} = 218.8 K_2 \sigma'^{0.5}_m \quad (5)$$

where K_2 is the parameter related to the shear strain.

Zhu et al.[11] examined the dynamic shear modulus and damping ratio of sand under a low strain through a resonant column test, established empirical formulas for E_{max}, E, G_{max} and G and modified Harden's formula via the Fujian saturated standard sand test. The maximum shear modulus was empirically formulated as

$$G_{max} = 580 \frac{(2.17 - e)^{2.2}}{(1 + e)} \sigma'_m \quad (6)$$

where e is the void ratio.

Through a resonant column test, Hardin and Drnevich[12] found that the dynamic shear modulus of sand decreases nonlinearly with the increasing shear strain. The dynamic shear modulus of sand was formulated as

$$G = G_{max} [1 - H(\gamma)] \quad (7)$$

$$H(\gamma) = \frac{|\gamma| / \gamma_\gamma}{1 + |\gamma| / \gamma_\gamma} \quad (8)$$

where γ is the shear strain, $|\gamma|$ is the absolute value of γ and γ_γ is the reference shear strain.

Ling et al.[13] studied the dynamic characteristics of a rock-fill dam through a large-scale static and dynamic triaxial test and found that the dynamic shear modulus and damping ratio were affected not merely by the confining pressure but also by the consolidation ratio. With the same dynamic shear strain, Guo et al.[14] found that the dynamic shear modulus with an initial deviator stress ratio of 0 is slightly higher than those with ratios of 0.43 and 0.75, with the latter two showing very small differences. The effect of the initial deviator stress ratio on the dynamic shear modulus was negligible compared with that of the mean effective consolidation stress. Moreover, the initial deviator stress ratio only had a slight effect on the damping ratio of loose sand, and this effect decreased along with an increasing mean effective consolidation stress. Liu et al.[15] studied the effects of void ratio and confining pressure on the dynamic deformation characteristics of filter materials by conducting a medium dynamic triaxial test and established a dynamic shear modulus formula that considers the influence of the void and confining stress ratios. Wang et al.[16] discussed the effects of the void ratio, confining pressure and vibration frequency on the dynamic shear modulus and damping ratio by performing dynamic triaxial and resonant column tests and found that both the void ratio and confining pressure significantly affect the dynamic shear modulus. Accordingly, they established a maximum shear modulus formula that takes the influence of the void ratio and confining pressure into account. In this formula, the maximum shear modulus decreases with an increasing water content and eventually stabilises. The changes in the dynamic shear modulus and damping ratios obtained from the dynamic triaxial and resonant column tests were consistent with those in the dynamic shear strain. He et al.[17] performed an electromagnetic dynamic triaxial test to examine the dynamic shear modulus characteristics of sand when the dynamic shear strain ranges between 10^{-6} and 10^{-2} and proposed a method for calculating the maximum dynamic shear modulus. They found that the dynamic shear modulus reaches its maximum value when the dynamic shear strain is less than 10^{-5}.

In sum, although the dynamic shear modulus and damping ratio of sand were widely studied, researchers mainly focused on small strains, while the effects of the initial shear stress and vibration frequency on the dynamic shear modulus remain unclear. Therefore, the dynamic shear modulus and damping ratio of sand under seismic loads and the influence of the initial shear stress and vibration frequency warrant further study, and a formula for computing dynamic shear modulus that takes the influence of the initial shear stress and vibration frequency into account should be established.

2 SOIL SAMPLES AND PLANS

2.1 Soil samples

Sand samples were collected from Wenchuan in the Sichuan Province, China, at a sampling depth of 5 m. **Table 1** shows the physical properties of the samples, and **Figure 1** displays the sand particle-size distribution curve.

Table 1: Physical properties of the test sand

Soil category	G_s	ρ_{dmax}	ρ_{dmin}	D_r	C_u	C_c
sand	2.66	1.67	1.22	55 %	3.5	0.64

2.2 Test procedures and methods

A dynamic triaxial testing system (DDS-70) and remoulded soil samples with a diameter of 39.1 mm and height of 80 mm were used in the test. **Figure 2** shows a photo of the dynamic triaxial testing system. The reconstituted specimens were prepared using a multilayer wet-mortar method, while vacuum pumping and revers-

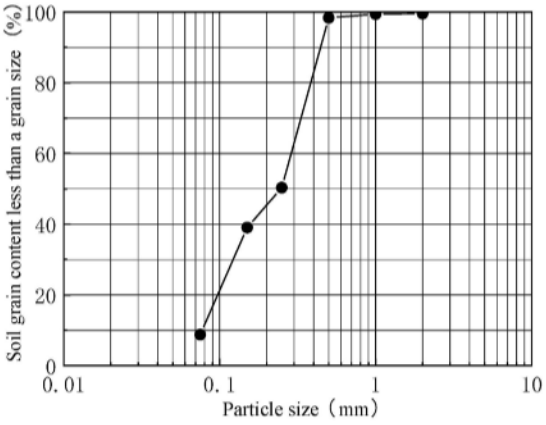

Figure 1: Particle size-distribution curve

ing pressure were applied to saturate the samples. When the pore water-pressure coefficient B is higher than or equal to 0.97, the saturation requirement is satisfied. When a sample was saturated, the drain valve was slowly opened. When the pore water-pressure dissipation approached 0, the drain valve was closed for 5 min. The consolidation was completed after the pore water-pressure stopped increasing. Anisotropic consolidation was conducted after completing the isobaric consolidation. In this process, the deviatoric stress was gradually increased, and the drain valve was opened. Consolidation was performed for a certain period when applied to the corresponding deviation stress. Afterwards, the drain valve was closed to complete the anisotropic consolidation. Due to the asymmetry and irregularity of seismic loading, which is a typical random dynamic load, it is impossible to repeat the earthquake with the same seismic waveform. Therefore, the seismic-loading input in this study is simulated with a sine wave of an equal amplitude waveform. The consolidation confining pressures in the tests are σ_c (50; 100; 150) kPa, the vibration frequencies are f are (1; 2; 3) Hz and the consolidation ratios (k_c) are 1.0, 1.2 and 1.4.

Figure 2: DDS-70 dynamic triaxial testing system

3 RESULTS AND ANALYSIS

The variation law of the dynamic shear modulus and damping ratio of saturated sand can serve as a reference for the design and analysis of structures. Therefore, these characteristics are examined from the aspects of the initial shear stress and vibration frequency.

3.1 Development of the dynamic shear modulus under different initial shear stresses

Figure 3 presents the relationship curves for G and γ when the consolidation ratios k_c are 1.0, 1.2 and 1.4. As the dynamic shear strain increases, the dynamic shear modulus obtained under different consolidation ratios shows a consistent decreasing trend. When the dynamic shear strain is lower than the turning point, the dynamic shear modulus shows a fast decay rate, but when the dynamic shear strain exceeds this turning point, the decay rate is reduced. Therefore, the dynamic shear strain of the turning point is defined as the threshold dynamic shear strain. **Figure 3** shows that the threshold dynamic shear strain is 0.05 % and it is not affected by the consolidation ratio. Moreover, the initial shear stress significantly influences the variation in the dynamic shear modulus with the dynamic shear strain. When the dynamic shear strain is constant, the dynamic shear modulus obviously increases with the initial shear stress. Regardless of whether the initial shear stress is applied or not, the dynamic shear modulus curve remains consistent with the decay rate of the dynamic shear strain at the beginning of the cycle, and the relationship between the dynamic shear modulus and dynamic shear strain is approximately linear. As the dynamic shear strain increases, the curve gradually becomes steady, and the difference between the dynamic shear modulus and dynamic shear strain is reduced under different initial shear stresses. Given that the soil particle skeleton tends

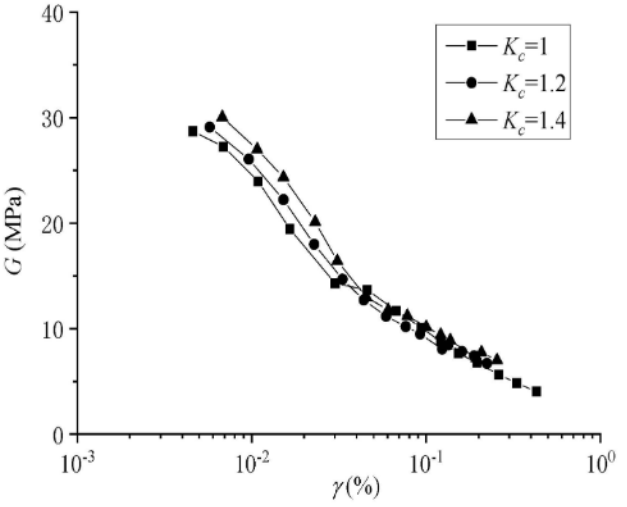

Figure 3: Relationship curves for G and γ under different initial shear stresses

to be more stable when a sample is subjected to the initial shear stress, a greater initial shear stress corresponds to a more stable skeleton. Moreover, as the initial shear stress greatly enhances the resistance of sand to shear deformation under a dynamic load, the dynamic shear modulus increases with the initial shear stress.

3.2 Development of the dynamic shear modulus under different vibration frequencies

Figure 4 shows the relationship curves for G and γ under different frequencies when σ_c = 150 kPa. The vibration frequency exerts a certain influence on the dynamic shear modulus of saturated sand under the same confining pressure. When the dynamic shear strain is lower than 0.05 %, the vibration frequency has a significant influence on the dynamic shear modulus of saturated sand. A higher vibration frequency corresponds to a greater dynamic shear modulus. When the dynamic shear strain exceeds 0.05 %, the influence of different vibration frequencies on the dynamic shear modulus is relatively small, and the dynamic shear modulus under different vibration frequencies increases with the dynamic shear strain and eventually becomes stable. A higher vibration frequency corresponds to a higher dynamic shear modulus-strain curve because under the same failure vibration frequency, a greater vibration frequency corresponds to a shorter cycle duration, and a shorter relative movement of soil particles and the surrounding free water increases the particle friction, consequently increasing the dynamic shear modulus of saturated sand.

3.3 Variation law of the dynamic shear modulus ratio

The dynamic stress/strain relationships of sand can be expressed with its dynamic stress/strain backbone curve under cyclic loading. The maximum dynamic stress and maximum dynamic shear strain, corresponding to each cycle under different dynamic loads are successively selected as the backbone points in the backbone curve, and then the dynamic stress/strain relationship backbone curve of sand and soil is obtained based on the smooth connection of each key point. The dynamic shear modulus E_d can be calculated based on the axial dynamic shear strain and axial dynamic stress obtained with the dynamic triaxial test, and then the dynamic shear modulus G can be obtained. The corresponding dynamic shear strain γ_d can be calculated with the axial dynamic shear strain ε_d, whereas the corresponding dynamic shear stress τ_d can be calculated with the axial dynamic stress σ_d as follows:

$$\begin{aligned} \gamma_d &= \varepsilon_d(1+\mu) \\ \sigma_d &= \frac{\sigma_d}{2} \\ G_d &= \frac{\tau_d}{\gamma_d} = \frac{E_d}{2(1+\mu)} \end{aligned} \tag{9}$$

where γ_d is the dynamic shear strain, ε_d is the axial dynamic shear strain, τ_d is the dynamic shear stress, σ_d is the axial dynamic stress, E_d is the dynamic shear modulus, G is the dynamic shear modulus and μ is Poisson's ratio.

According to Equation (9), the maximum dynamic shear modulus can be expressed as

$$G_0 = \frac{E_d}{2(1+\mu)} \tag{10}$$

where G_0 is the maximum dynamic shear modulus and E_0 is the initial dynamic shear modulus.

Equation (9) suggests that when converting between the dynamic shear strain and dynamic shear strain, the dynamic shear modulus and dynamic shear modulus, Poisson's ratio of saturated sand should be determined. Lambe et al.[18] stated that Poisson's ratio has no obvious influence on the dynamic shear modulus. In this study, Poisson's ratio of saturated sand was set to 0.35.

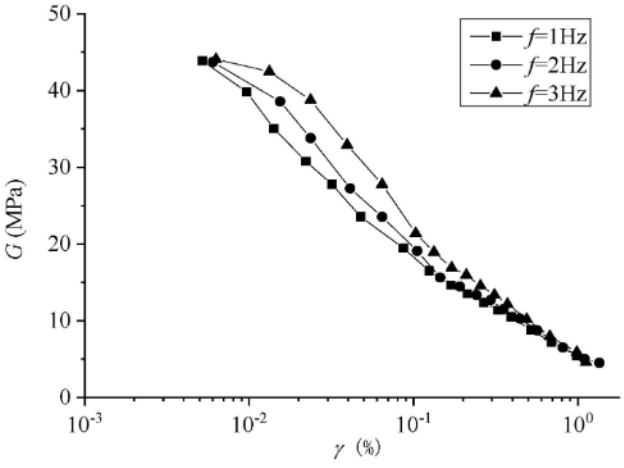

Figure 4: Relationship curves for G and γ under different vibration frequencies (σ_c = 150 kPa)

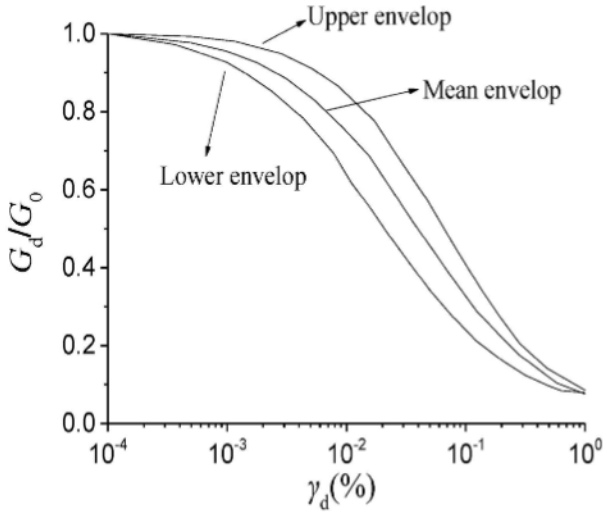

Figure 5: Variation law of the normalised dynamic shear modulus/shear strain proposed by Seed

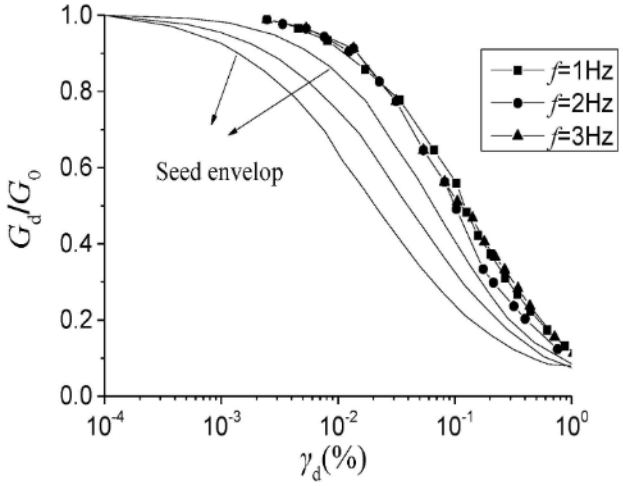

Figure 6: Dynamic shear strain/dynamic shear modulus curves under different vibration frequencies

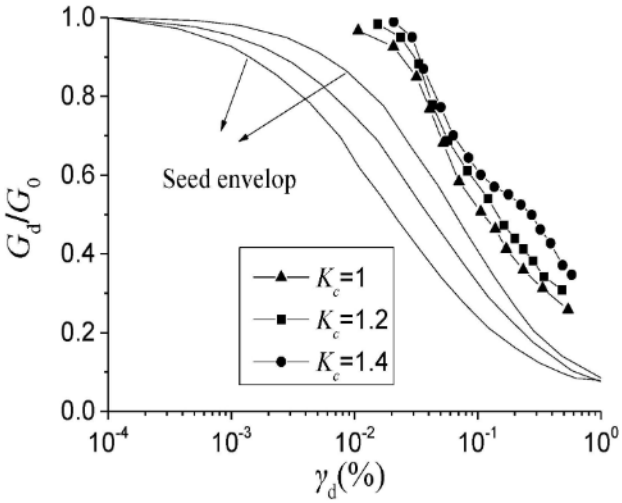

Figure 8: Dynamic shear strain/dynamic shear modulus curves under different initial shear stresses

The dynamic shear strain can be converted into dynamic shear strain and the dynamic shear modulus can be converted into dynamic shear modulus using Equation (9). The normalised dynamic shear modulus G/G_0 can be obtained from dynamic shear modulus G divided by initial dynamic shear modulus G_0, and then the normalised dynamic shear modulus/shear strain curves can be obtained. Consequently, the normalised dynamic shear modulus can be studied under different initial shear stresses and frequencies.

Seed and Idriss[10] built their normalised dynamic shear modulus/shear strain curves based on a large amount of soil-measurement data as shown in **Figure 5**. The upper, lower and mean envelopes were also identified. The normalised dynamic shear modulus obtained from the test data was distributed in the interval between the upper and lower envelopes, and the middle curve of the envelope line represents the mean envelope.

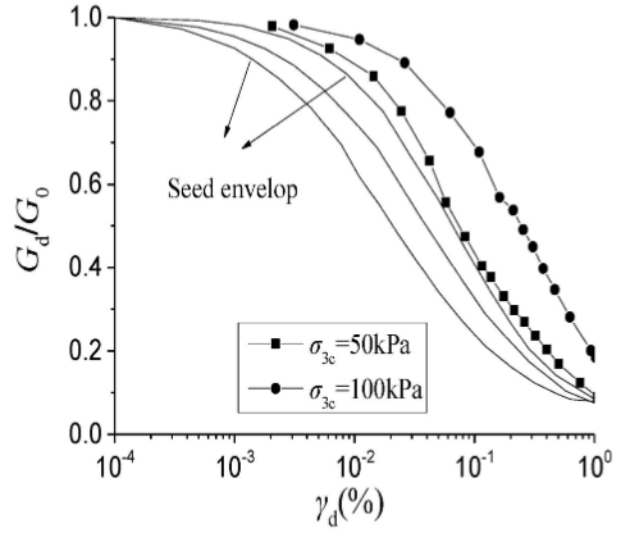

Figure 7: Dynamic shear strain/dynamic shear modulus curves under different confining pressures(f = 2 Hz

Figure 6 shows the upper, lower and mean envelopes proposed by Seed and the normalised dynamic shear modulus/shear strain curves under different frequencies when the confining pressure is 50 kPa. The normalised dynamic shear modulus/shear strain curves of saturated sand are located above the Seed envelope. Moreover, the normalised dynamic shear modulus/shear strain curves under different frequencies fall into a narrow range and land near the Seed upper envelope. Only the vibration frequency has a slight effect on these curves.

Figure 7 shows the normalised dynamic shear modulus/shear strain curves under different confining pressures when the vibration frequency is 2 Hz. The curves under different confining pressures also fall into a narrow range. Results show that a curve changes with the confining pressure. Specifically, a greater confining pressure corresponds to a higher normalised dynamic shear modulus.

Figure 8 shows the normalised dynamic shear modulus/shear strain curves under different initial shear stresses. A greater initial shear stress corresponds to a higher curve. In other words, the initial shear stress has a significant influence on the dynamic shear modulus of saturated sand.

3.4 Establishment of a dynamic shear modulus ratio equation

A normalised dynamic shear modulus/shear strain curve can be simulated by hyperbolic, exponential and probability curves. Harden and Drnevich proposed the H-D model for calculating the dynamic shear modulus of soil through resonant column and cyclic simple shear tests. The dynamic shear modulus was calculated as

$$G_d = G_0\left(1-\frac{\frac{\gamma}{\gamma_r}}{1+\frac{\gamma}{\gamma_r}}\right)=G_0\left(\frac{1}{1+\frac{\gamma}{\gamma_r}}\right) \quad (11)$$

Meanwhile, function $H(\gamma)$ can be defined as

$$H(\gamma)=\frac{\frac{\gamma}{\gamma_r}}{1+\frac{\gamma}{\gamma_r}} \quad (12)$$

Where γ_r is the reference shear strain.

Some researchers argue that substituting $\gamma_{0.5}$ for γ_r will reduce the dispersion of data and that the categories of soil, test methods and confining pressure have no effects on the normalised dynamic shear modulus/shear strain curves.[19–21]

The Davidenkov model can well describe the relationship between the dynamic shear stress and dynamic shear strain. The function of this model can be formulated as

$$H(\gamma)=\left[\frac{\left(\frac{\gamma}{\gamma_0}\right)^{2B}}{1+\left(\frac{\gamma}{\gamma_0}\right)^{2B}}\right]^A \quad (13)$$

where A, B and γ_0 are the dynamic parameters of soil. When A = 1.0 and B = 0.5, the Davidenkov model degrades into the H-D model. Given that the Davidenkov model selects three parameters that can describe the normalised dynamic shear modulus/shear strain curves and outperform the H-D model with only one parameter, the fitting curves of the normalised dynamic shear modulus/dynamic shear strain are more suitable for the Davidenkov model than for the H-D model.

Given that the H-D model only provides the reference shear strain to reflect the soil parameters, the test results are highly discrete and the normalised dynamic shear modulus/shear strain curves cannot be accurately reflected, especially in a range of 10^{-4} to 10^{-3}, which is the same range as for the shear strain amplitudes resulting from moderate or higher-intensity earthquakes. Meanwhile, the Davidenkov model is difficult to interpret because of its large number of parameters, and the relationship between the normalised dynamic shear modulus and shear strain differs according to the consolidation confining pressure.

On the basis of the test results, Equation (11) was changed to

$$\frac{G}{G_0}=\frac{1}{1+\left(\frac{\gamma}{\gamma_r}\right)^m} \quad (14)$$

where γ_r is the reference shear strain and m is the dynamic parameter of sand.

The γ_r and m values of saturated sand obtained from the test under different vibration frequencies are shown in **Table 2**.

Table 2: γ_r and m values under different vibration frequencies

Vibration frequency(Hz)	1		2		3	
Confining pressure (kPa)	m	$\gamma_r \times 10^{-3}$	m	$\gamma_r \times 10^{-3}$	m	$\gamma_r \times 10^{-3}$
50	1.40	1.42	0.87	0.78	0.9	1.14
100	0.97	2.11	0.83	2.27	0.97	2.52
150	1.15	2.62	1.13	2.25	1.19	2.78

The γ_r and m values of saturated sand obtained with the test under different initial shear stresses when f = 1 Hz are shown in **Table 3**.

Table 3: γ_r and m values under different initial shear stresses when f = 1Hz

Consolidation ratio	1		1.2		1.4	
Confining pressure (kPa)	m	$\gamma_r \times 10^{-3}$	m	$\gamma_r \times 10^{-3}$	m	$\gamma_r \times 10^{-3}$
50	1.40	1.42	0.92	0.84	1.4	0.9
100	0.97	2.11	1.12	2.42	0.88	1.57
150	1.15	2.62	0.81	1.75	0.80	1.13

Experimental results show that γ_r and m differ under the same frequency and varying confining pressures, under the same confining pressure and varying frequencies or under the same confining pressure and varying initial shear stresses. Therefore, Equation (14) was used to express the relationship between the normalised dynamic shear modulus and dynamic shear strain, which can better reflect the influence of different confining pressures, frequencies and initial shear stresses. Fitting results suggest that this equation shows good agreement with the test data and has good applicability.

3.5 Determination of the damping ratio

The variation in the soil damping ratio is often expressed by the relationship between the damping ratio and dynamic shear strain. The damping ratio of soil is defined as

$$\lambda=\frac{\Delta W}{4\pi W} \quad (15)$$

where ΔW is the energy lost in one cycle and W is the total energy.

Seed and Idriss initially established a relationship between the damping ratio and dynamic shear strain, and then Hardin and Drnevich performed a comparative analysis of the geometric characteristics of the stress/strain hysteresis loop based on the experimental data and established the following relationship between the damping ratio and dynamic shear modulus:

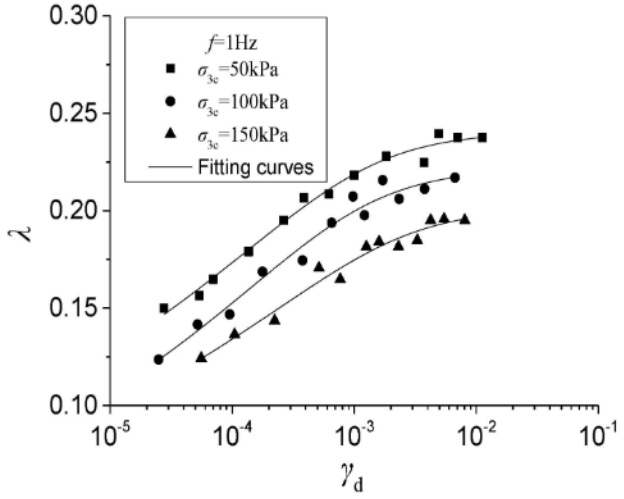

Figure 9: Variation curves of damping ratio with dynamic shear strain under different confining pressures

$$\lambda = \lambda_{max}\left(1-\frac{G_d}{G_0}\right) \tag{16}$$

where λ_{max} is the maximum damping ratio.

By combining Equations (11) and (16), the relationship between the damping ratio and dynamic shear strain can be expressed as

$$\lambda = \lambda_{max}\left(\frac{\frac{\gamma_d}{\gamma_r}}{1+\frac{\gamma_d}{\gamma_r}}\right)^n \tag{17}$$

where λ_{max} is the maximum damping ratio, γ_r is the reference shear strain and n is the parameter of sand.

3.6 Variation laws of the damping ratio

Considering the dispersion of the damping ratio test data, those abnormal points where the damping ratio changes greatly were removed. **Figure 9** shows the variation curves of the damping ratio with shear strain under different confining pressures. The damping ratio increases with dynamic shear strain. At the same strain level, a greater confining pressure corresponds to a smaller damping ratio. When the strain amplitude is small, the damping ratio is close to zero and is less affected by the load applied. The fitting parameters of Equation (17) obtained with the test are shown in **Table 4.**

Table 4: Fitting-parameter values

Vibration frequency (Hz)	1		
Confining pressure (kPa)	λ_{max}	m	$\gamma_r \times 10^{-4}$
50	0.24	0.13	9.93
100	0.22	0.16	9.03
150	0.20	0.13	17.9

Given the large strain of the dynamic triaxial test, the damping ratio/dynamic shear strain curves are relatively flat. Moreover, considering the limited number of experiments and the large dispersion, the damping ratio/dynamic shear strain curves represent only an average trend. For major engineering sites, detailed tests should be performed to determine the dynamic performance parameters of soil. The empirical formulas and parameters presented in this paper can be used as references.

Figure 10 shows the variation curves of the damping ratio with dynamic shear strain under different initial shear stresses. The initial shear stress shows a significant influence on the damping ratio of saturated sand. A

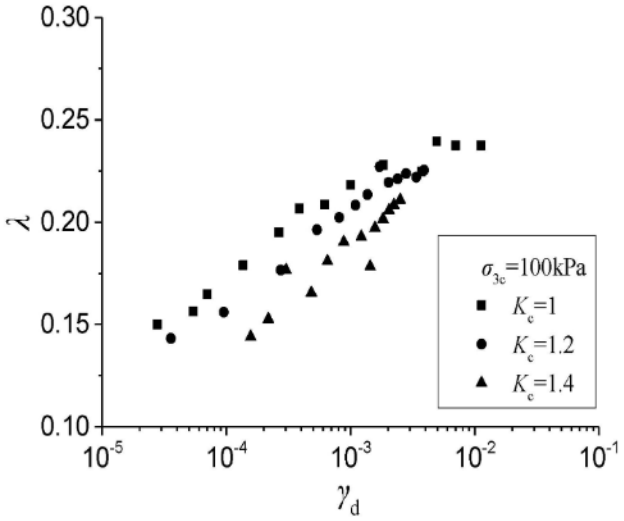

Figure 10: Variation curves of damping ratio with dynamic shear strain under different initial shear stresses

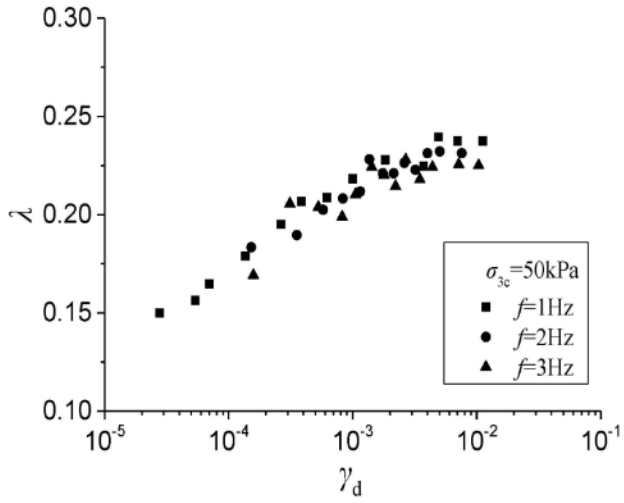

Figure 11: Variation curves of damping ratio with dynamic shear strain under different vibration frequencies

greater initial shear stress corresponds to a smaller damping ratio.

Figure 11 shows the variation curves of damping ratio with dynamic shear strain under different vibration frequencies. The influence of the vibration frequency on damping ratio is not obvious. The data points with low frequencies are above the ones with high frequencies. The damping ratio shows a decreasing trend with the increasing frequency and the difference becomes more obvious when the dynamic shear strain exceeds 0.5 %.

4 CONCLUSIONS

This study utilises a dynamic triaxial test system to examine the dynamic shear modulus and damping ratio of the saturated sand from Wenchuan to understand the influence of the initial shear stress and vibration frequency on the dynamic shear modulus and damping ratio of sand and to establish the normalised dynamic shear modulus equation that takes the initial shear stress and vibration frequency into consideration. The following conclusions were obtained:

(1) A threshold dynamic shear strain can be observed in saturated sand. When the dynamic shear strain is lower than the threshold dynamic shear strain, the dynamic shear modulus shows a fast decay rate. However, such a decay rate is reduced when the dynamic shear strain exceeds the threshold value.

(2) The initial shear stress and vibration frequency significantly affect the dynamic shear modulus of saturated sand. When the dynamic shear strain is lower than the threshold dynamic shear strain, the dynamic shear modulus significantly increases with the initial shear stress and vibration frequency. However, when the dynamic shear strain exceeds the threshold value, the effect of the initial shear stress and vibration frequency gradually increases and eventually stabilises.

(3) The vibration frequency only has a slight influence on the normalised dynamic shear modulus/shear strain curves. The dynamic shear strain/normalised dynamic shear modulus curves under different frequencies are generally within the same band and fall near the Seed upper envelope. Meanwhile, the initial shear stress significantly affects these curves where a greater initial shear stress corresponds to a higher curve.

(4) A formula for the normalised dynamic shear modulus/strain that takes the initial shear stress and vibration frequency into consideration is established based on the analysis results. Fitting results show that this formula agrees well with the test data and has good applicability.

(5) The initial shear stress significantly affects the damping ratio. A larger initial shear stress corresponds to a smaller damping ratio. The vibration frequency only has a small influence on the damping ratio.

Acknowledgments

The authors are grateful for the support by the Qing Lan Project, the research project of the Ministry of Housing and Urban-Rural Development (No. 2019-K-131), the research project of Nanjing Scientific Construction System (No. Ks2039) and the research project of the Nanjing Vocational Institute of Transport Technology (No. JZ2001).

5 REFERENCES

[1] K. Pan, Z. X. Yang, Effects of initial static shear on cyclic resistance and pore pressure generation of saturated sand, Acta Geotechnica, 13 (**2018**) 5, 473–487, doi:10.1007/s11440-017-0614-5

[2] Y. Feng, W. Zhang, Experimental study on stress-water content-strain relationship of remolded loess under directional shear stress path, Journal of Qinghai University, 36 (**2018**) 1, 47–53

[3] Z. L. Zhou, G. X. Chen, Q. Wu, Effect of initial static shear stress on liquefaction and large deformation behaviors of saturated silt, Yantu Lixue/Rock & Soil Mechanics, 38 (**2017**) 5, 1314–1320, doi:10.11779/CJGE201603014

[4] Z. X. Yang, K. Pan, Flow deformation and cyclic resistance of saturated loose sand considering initial static shear effect, Soil Dynamics & Earthquake Engineering, 92 (**2017**), 68–78, doi:10.1016/j.soildyn.2016.09.002

[5] Z. H. Zhang, X. C Huang, Q.T. Bi, Effect of initial shear stress and phase difference on dynamic characteristics of saturated sand, Yangtze River, 48 (**2017**) 3, 70–74

[6] G. Suazo, A. Fourie, J. Doherty, Effects of confining stress, density and initial static shear stress on the cyclic shear response of fine-grained unclassified tailings, Geotechnique, 66 (**2016**) 5, 1–12, doi:10.1680/jgeot.15.P.032

[7] J. Wang, P. Luo, F. Y. Liu, Effect of angle between directions of initial shear stress and cyclic load on softening properties of soft clay, Chinese Journal of Rock Mechanics and Engineering, 35 (**2016**) 5, 1072–1080, doi:10.13722/j.cnki.jrme.2015.1182

[8] J. T. Cao, Experimental study on dynamic behaviors of Wenchuan earthquake area saturated sand under cyclic loading, Hohai University, Nanjing 2014

[9] B. Hardin, F. E. Richart, Elastic wave velocities in granular soils, Journal of the Soil Mechanics and Foundations Division, 89 (**1963**) 1, 603–624, doi:10.1061/JSFEAQ.0000493

[10] H. B. Seed, I. M. Idriss, Soil moduli and damping factors for dynamic response analyses, Earthquake Engineering Research Center, University of California, Berkeley 1970

[11] L. G. Zhu, X. F. Wu, A study of dynamic properties of sand under the low amplitude strain, Hydropower Automation & Dam Monitoring, 12 (**1988**) 1, 27–33

[12] B. O. Hardin, V. P. Drnevich, Shear Modulus and Damping in Soils, J. of the Soil Mechanics and Foundations Div. – ASCE, 98 (**1972**) 6, 667–692

[13] H. Ling, H. Fu, Experimental study on dynamic deformation characteristics of dam materials, Chinese Journal of Rock Mechanics and Engineering, 25 (**2006**) 2, 4059–4064

[14] Y. Guo, M. T. Luan, Experimental study on effect of initial stress condition on dynamic behavior and deformation parameters of loose sands, Rock and Soil Mechanics, 26 (**2005**) 8, 1195–1120

[15] H. L. Liu, G. Yang, Y. M. Chen, Experimental study of factors influencing dynamic shear modulus and damping ratio of dam inverted filler, Rock and Soil Mechanics, 31 (2010) 7, 2030–2034

[16] B. H. Wang, G. X. Chen, Q. X. Hu, Experiment of dynamic shear modulus and damping of Nanjing fine sand, World Earthquake Engineering, 26 (**2010**) 3

[17] C. R. He, Dynamic Triaxial Test on Modulus and Damping, Chinese Journal of Geotechnical Engineering, 19 (**1997**) 2, 39–48

[18] T. W. Lambe, R .V. Whiteman, Soil Mechanics, John Wiley and Sons, New York 1969

[19] T. Teachavorasinskun, Stiffness and Damping of Sands in Torsion Shear, Proc. 2nd. Int. Conf. on Recent Adv. in Geot. Earthq. Engrg. & Soil Dyn, 1991

[20] M. Kanatani, K. Nishi, M. Ohnami, K. Keikaku, H. Namita, Numerical Simulation of Shaking Table Test by Nonlinear Response Analysis Method, Proc. 2nd 1nt. Conf. on Recent Adv. in Geot. Earthq, Eng. & Soil Dyn., 1991

[21] P. P. Marin, H. B. Seed, One-Dimensional Dynamic Ground Response Analyses, Journal of the Geotechnical Engineering Division, 108 (1982) 7, 935–954, doi:10.1061/AJGEB6.0001316